FEBS Letters 582 (2008) 1141–1146

An urokinase receptor antagonist that inhibits cell migration by blocking the formyl peptide receptor

Katia Bifulco[a], Immacolata Longanesi-Cattani[a], Lucia Gargiulo[a,1], Ornella Maglio[b], Mauro Cataldi[c], Mario De Rosa[d], Maria Patrizia Stoppelli[e], Vincenzo Pavone[b], Maria Vincenza Carriero[a,*]

[a] *Department of Experimental Oncology, National Cancer Institute of Naples, via M. Semmola, 80131 Naples, Italy*
[b] *Department of Chemistry,"Federico II" University of Naples, Naples, Italy*
[c] *Division of Pharmacology, Department of Neuroscience, "Federico II" University of Naples, Naples, Italy*
[d] *Department of Experimental Medicine, Second University of Naples, Naples, Italy*
[e] *Institute of Genetics and Biophysics "Adriano Buzzati-Traverso", Naples, Italy*

Received 18 December 2007; revised 2 March 2008; accepted 4 March 2008

Available online 11 March 2008

Edited by Veli-Pekka Lehto

Abstract **Urokinase receptor (uPAR) plays a key role in physiological and pathological processes sustained by an altered cell migration. We have developed peptides carrying amino acid substitutions along the Ser^{88}-Arg-Ser-Arg-Tyr^{92} (SRSRY) uPAR chemotactic sequence. The peptide pyro glutamic acid (pGlu)-Arg-Glu-Arg-Tyr-NH2 (pERERY-NH_2) shares the same binding site with SRSRY and competes with *N*-formyl-Met-Leu-Phe (fMLF) for binding to the G-protein-coupled *N*-formyl-peptide receptor (FPR). pERERY-NH_2 is a dose-dependent inhibitor of both SRSRY- and fMLF-directed cell migration, and prevents agonist-induced FPR internalization and fMLF-dependent ERK1/2 phosphorylation. pERERY-NH_2 is a new and potent uPAR inhibitor which may suggest the generation of new pharmacological treatments for pathological conditions involving increased cell migration.**

Keywords: Inhibitors of Cell Migration; Formyl-peptide receptor; Urokinase receptor

1. Introduction

Cell migration contributes to several diseases driven by aberrant cell motility, such as chronic inflammation, vascular disease and tumor metastasis [1,2]. The receptor for the urokinase-type plasminogen activator (uPAR) plays an important role in physiological processes such as wound healing, inflammation and stem cell mobilization, and in severe pathological conditions such as tumour invasion and metastasis [3]. uPAR is a three domains (D1, D2 and D3) protein anchored to the cell membrane with a glycosyl–phosphatidyl–inositol [4]. uPAR can form a complete signalling unit only when associated with transmembrane receptors, such as G-protein-coupled receptors [5–8]. The uPAR engagement with uPA favours the exposure of the chemotactic Ser^{88}-Arg-Ser-Arg-Tyr^{92} sequence which belongs to a flexible linker connecting the uPAR domains D1 and D2 [9,10]. Residues 91–94 are conserved across species [11]. Through Ala-scan, we have found that both Arg residues of the peptide H-Ser-Arg-Ser-Arg-Tyr-OH (SRSRY) are essential to any signalling activity [12]. SRSRY promotes cytoskeletal rearrangements and directional cell migration by binding to the low (FPRL1) or the high *N*-formyl-peptide receptor (FPR) affinity formyl peptide receptors [12–14].

We have developed a series of synthetic peptides carrying specific amino acid substitutions along the SRSRY sequence. In this article, we report that the peptide pyro glutamic acid (pGlu)-Arg-Glu-Arg-Tyr-NH_2 (pERERY-NH_2) prevents SRSRY chemotactic activity by antagonizing the G-protein-coupled FPR.

2. Materials and methods

2.1. Peptide synthesis and purification

Peptides were synthesized by the solid phase approach using standard Fmoc methodology in a manual reaction vessel [15]. Peptides were purified by a RP-HPLC C18 column (Vydac 218TP1010) to a 99% purity, as determined by analytical RP-HPLC. Molecular weights were confirmed by mass spectrometry.

2.2. Cell cultures

Human Embryonic Kidney HEK-293, Rat Basophilic Leukemia RBL-2H3, and RBL-2H3/ETFR [16] cells were grown in DMEM supplemented with 10% FBS, 100 IU/ml penicillin and 50 μg/ml streptomycin.

2.3. Motility assays

Cell migration assays were performed in modified Boyden chambers for 4 h or in Dunn chambers for 6 h as previously described [12,17].

2.4. Binding assay

Five micrograms recombinant $D2_{(88–183)}$ uPAR fragment (Calbiochem) were biotinylated using a kit purchased from Amersham according to the manufacturer's recommendations. HEK-293 cells (1×10^6) were harvested, incubated with or without the indicated effectors for 15 min at 23 °C and then exposed to biotinylated $D2_{(88–183)}$ diluted in binding buffer (DMEM containing 1 mg/ml BSA) for 2 h at 4 °C.

*Corresponding author. Fax: +39 0815903814.
E-mail address: mariolinacarriero@yahoo.it (M.V. Carriero).

[1]Present Address: Department of Haematology, Imperial College, Faculty of Medicine, London, United Kingdom.

Abbreviations: uPAR, urokinase receptor; pGlu, pyro glutamic acid; fMLF, *N*-formyl-Met-Leu-Phe; FPR, *N*-formyl-peptide receptor

0014-5793/$34.00
doi:10.1016/j.febslet.2008.03.001

Surface-associated biotinylated proteins were eluted with an acid buffer [18], separated onto a 12.5% SDS–PAGE, and analysed for the biotin content by Western blot.

2.5. Fluorescence microscopy

Cells, grown on glass slides to semi-confluence, were incubated with diluents, or the indicated effectors, for 60 min at 4 °C or 30 min at 37 °C. Then, cells were washed with PBS, exposed to *N*-formyl-Nle-Leu-Phe-Nle-Tyr-Lys fluorescein (Molecular Probes) for additional 60 min at 4 °C or 30 min at 37 °C and analysed by a Zeiss LMS510 confocal microscope. Image analysis and quantization of the cell-associated fluorescence were performed on 100 cells, recorded in two different experiments, by using the Axio Vision 4.4 software (Carl Zeiss).

2.6. ERK1/2 phosphorylation assay

Cell lysates were prepared with RIPA buffer and cleared by centrifugation as previously reported [12]. Fifty micrograms of proteins/sample were separated on a 10% SDS–PAGE, and transferred to a nitrocellulose membrane. Western blot analysis was performed using 2 μg/ml anti-phospho-ERK1/2 polyclonal antibody. Total ERK1/2 was assessed by re-probing filters with 2 μg/ml anti-ERK1 and anti-ERK2 monoclonal antibodies. Densitometry of autoradiographic bands, was performed by NIH (Bethesda, MD) Image 1.62 software.

2.7. Cytosolic Ca^{2+} measurement

Changes in intracellular Ca^{2+} levels were measured observing with a confocal Zeiss LSM510 microscope (excitation: 488 nm, emission band pass: 500–550) single cells loaded with 5 μM fluo-3AM (Invitrogen-Molecular Probes) for 45 min at 37 °C in humidified air containing 5% CO_2, and continuously perfused with Krebs solution (160 mM NaCl, 5 mM KCl, 10 mM glucose, 10 mM Hepes, 1.2 mM $MgCl_2$, 1.5 mM $CaCl_2$, pH 7.4), with or without the peptide under investigation. Offline analysis was performed using the Image J1.37 software (http://rsb.info.nih.gov/ij/index.html) and the Time series analyzer plug-in (http://rsb.info.nih.gov/ij/plugins/time-series.html).

2.8. Statistical analysis

The results were analysed using the Student's *t*-test. A value of $P < 0.001$ was considered to be significant.

3. Results

3.1. Selection of pERERY-NH_2 as an antagonist of the SRSRY-directed cell migration

As a first approach, five Glu-scanned SRSRY peptides were synthesized and tested for their ability to promote or to prevent directional cell migration in Boyden chambers. Since all peptides failed to promote HEK-293 cell migration up to 100 nM concentration (not shown), we tested their ability to inhibit SRSRY-dependent cell migration. As expected, HEK-293 cells responded to SRSRY motogen stimulus (280% of the basal migration) [12]. Interestingly, the addition to the lower chamber of equimolar concentrations of H-Ser-Arg-Glu-Arg-Tyr-OH and SRSRY, caused a 31% inhibition of HEK-293 cell migration (Table 1), while the other peptides were ineffective. This finding suggested that the Arg-Glu-Arg central core may be relevant to the inhibition of the SRSRY-dependent cell migration. Therefore, the SRSRY double mutants listed in Fig. 1A were tested for their ability to inhibit SRSRY-dependent HEK-293 cell migration. While the control peptide H-Ala-Arg-Ala-Arg-Tyr-OH (ARARY) did not exert any effect, pGlu-Arg-Glu-Arg-Tyr-OH and H-Glu-Arg-Glu-Arg-Tyr-OH, caused, at 100 pM concentration, a 45% and a 30% inhibition, respectively (Fig. 1A). Furthermore, the C-terminal amidated peptide pGlu-Arg-Glu-Arg-Tyr-NH_2 (pERERY-NH_2) triggered a 70% inhibition at 100 pM concentration (Fig. 1A). Further characterization of pERERY-NH_2 shows that this peptide inhibited SRSRY-directed HEK-293 cell migration in a dose-dependent manner. Inhibition starts at 100 fM concentration, 50% of maximal effect being reached at 100 pM. Maximal inhibition was reached in the nM range (Fig. 1B).

Table 1
Effects of SRSRY-derived Glu-substituted peptides on SRSRY-directed HEK-293 cell migration

Peptides (10 nM)	Cell migration
None	100 ± 7
H-Glu-Arg-Ser-Arg-Tyr-OH	99 ± 5
H-Ser-Glu-Ser-Arg-Tyr-OH	101 ± 1
H-Ser-Arg-Glu-Arg-Tyr-OH	69 ± 2
H-Ser-Arg-Ser-Glu-Tyr-OH	98 ± 4
H-Ser-Arg-Ser-Arg-Glu-OH	100 ± 8

Chemotactic response of HEK-293 cells to 10 nM SRSRY in a Boyden chamber assay in the presence or in the absence of 10 nM substituted peptides. SRSRY-dependent cell migration (280% of the basal migration) was considered as 100% and cell migration in the presence of substituted peptides was calculated as a percentage of that. Data points are the means ± S.D. of three independent experiments.

3.2. pERERY-NH_2 antagonizes FPR signalling

It is known that $D2_{(88–183)}$ uPAR fragment binds to FPR or FPRL1 through the SRSRY sequence [12–14]. To assess whether pERERY-NH_2 and SRSRY share the same binding site, HEK-293 cells were pre-incubated with an excess unlabeled $D2_{(88–183)}$, SRSRY, pERERY-NH_2 or ARARY, and then exposed to biotinylated $D2_{(88–183)}$. Eluted proteins were analysed for their biotin content by Western blot. All effectors, with the exception of ARARY, prevented the binding of biotinylated $D2_{(88–183)}$ to cell surface to a similar extent, suggesting that both SRSRY and pERERY-NH_2 recognize the same cell surface receptor (Fig. 2A). A likely possibility is that pERERY-NH_2 recognizes FPR which is constitutively expressed by HEK-293 cells [14]. To study the role of FPR, we took advantage of RBL-2H3 cells which are devoid of FPR and RBL-2H3/ETFR which stably express FPR [16]. In a migration assay toward *N*-formyl-Met-Leu-Phe (fMLF), we found that pERERY-NH_2 inhibits RBL-2H3/ETFR cell migration in a dose-dependent manner (Fig. 2B). The inhibitory effect starts at 10 fM concentration, 50% of maximal effect being reached at 1 pM. Maximal inhibition is reached in the low nM range (Fig. 2B). Unlike RBL-2H3 cells, RBL-2H3/ETFR cells move toward SRSRY and fMLF, the extent of cell migration being reduced to the basal levels by 100 pM pERERY-NH_2 (Fig. 2C). In contrast, RBL-2H3 and RBL-2H3/ETFR cell response to fibronectin (Fn) [16] was not prevented by pERERY-NH_2 (Fig. 2C). This indicates that antagonistic effect of pERERY-NH_2 is directed to SRSRY signalling and it is mediated by FPR. To gain some insights into the cellular effects of pERERY-NH_2, RBL-2H3/ETFR cells were grown adherent onto a glass slide, exposed to a 10 nM fMLF gradient containing 100 pM pERERY-NH_2 or diluents in a DUNN chamber for 6 h, and then stained with rhodamine–phalloidin. Cells subjected to the fMLF gradient exhibited an elongated morphology and recognisable aligned protrusions associated to locomotion in the 80% cell population. Vice versa, the addition of pERERY-NH_2 to the fMLF gradient reduced cell elon-

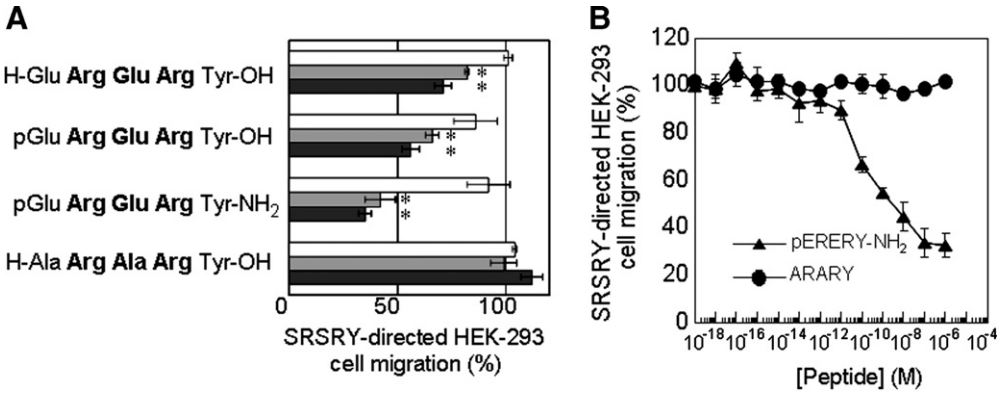

Fig. 1. Screening of peptide inhibitors of the SRSRY-directed cell migration. HEK-293 cells were allowed to migrate in Boyden chambers toward 10 nM SRSRY in combination with 100 fM (□), 100 pM (■), or 100 nM (■) or increasing concentration of the indicated peptides. The extent of cell migration in the presence of the peptides was expressed as a percentage of the SRSRY-dependent directional cell migration assessed in the absence of peptides, considered as 100%. Data represent the means ± S.D. of three (A, $^{*}P < 0.0001$ compared to SRSRY-dependent directional cell migration) or four (B) independent experiments performed in duplicate.

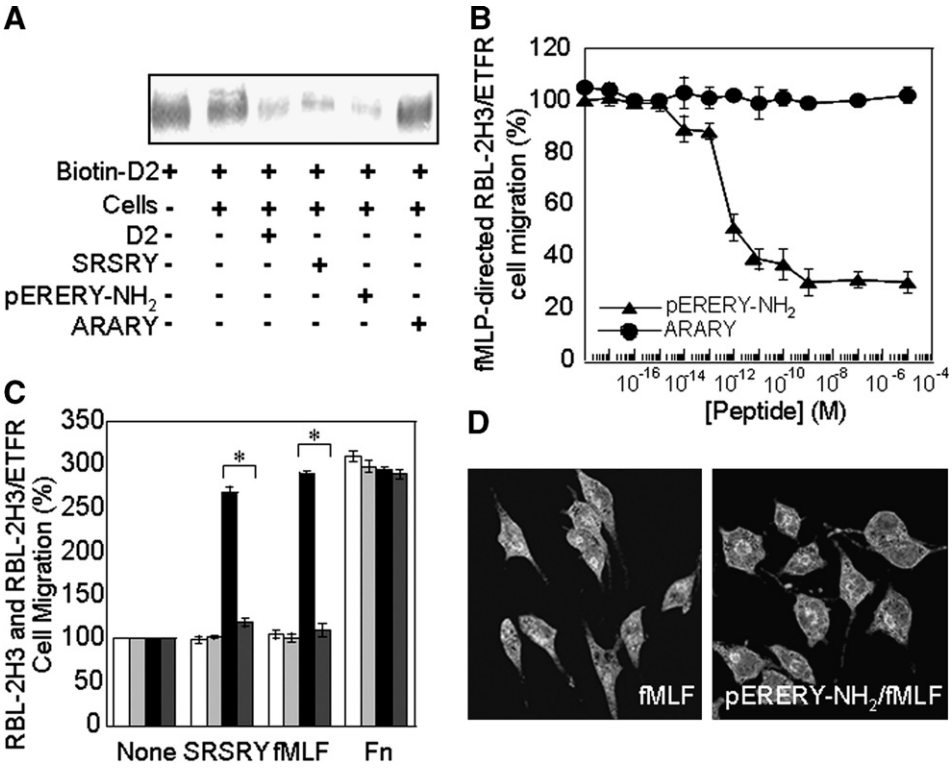

Fig. 2. FPR-dependence of pERERY-NH_2 inhibitory effect. (A) HEK-293 cells were incubated with 500 nM $D2_{(88–183)}$, 500 nM SRSRY, 500 nM pERERY-NH_2, 500 nM ARARY, or diluents and subsequently exposed to 100 nM biotinylated $D2_{(88–183)}$. Cell surface-associated proteins were eluted and subjected to Western blot analysis. Five microlitres of biotinylated $D2_{(88–183)}$ was loaded as a control. (B) Dose-dependent effect of pERERY-NH_2 and ARARY on RBL-2H3/ETFR cell migration directed to 10 nM fMLF. The extent of cell migration was expressed as a percentage of the fMLF-dependent directional cell migration in the absence of peptides (100%). The data represent the means ± S.D. of three independent experiments performed in duplicate. (C) Chemotactic response of RBL-2H3 (□, ■), or RBL-2H3/ETFR (■, ■) cells to 10 nM SRSRY, 10 nM fMLF or 50 μg/ml fibronectin (Fn), in the presence (■, ■) or in the absence (□, ■) of 100 pM pERERY-NH_2. The extent of cell migration was expressed as a percentage of the random cell migration assessed in the absence of chemoattractant, considered as 100% (none). The data represent the means ± S.D. of independent experiments performed in duplicate ($^{*}P < 0.0001$). (D) Representative images of rhodamine–phalloidin stained RBL-2H3/ETFR cells subjected in a DUNN chamber to a 10 nM fMLF chemotactic gradient, in the absence or in the presence of 100 pM pERERY-NH_2. Original magnification: 100×.

gation and alignment with the appearance of F-actin linear distribution along the plasma membranes in at least 75% of cell population (Fig. 2D). Taken together, these data indicate that FPR-mediated pERERY-NH_2 inhibitory effect involves a marked inhibition of cytoskeletal re-organization occurring during locomotion.

In response to agonist-stimulation, many GPCRs, including FPR, are internalized [19,20]. We first evaluated the direct

binding of pERERY-NH_2 to RBL-2H3/ETFR cells. Cells were pre-incubated at 4 °C with 100 nM fMLF, 100 nM ARARY or increasing concentrations of pERERY-NH_2 and then exposed to *N*-formyl-Nle-Leu-Phe-Nle-Tyr-Lys-fluorescein. As expected, RBL-2H3 cells did not bind to the fluorescent fMLF analog (not shown). However, pERERY-NH_2 specifically inhibited binding of fluorescent agonist to RBL-2H3/ETFR cells in a dose-dependent manner and to a similar extent than fMLF (Fig. 3A). Quantization of the cell-associated fluorescence revealed that, whereas 100 fM pERERY-NH_2 was ineffective, pERERY-NH_2 at 100 pM, 10 nM or 10 μM concentrations caused a 72%, 98% and 94% reduction of ligand binding, respectively. Then, to evaluate the effect of pERERY-NH_2 on agonist-dependent FPR internalization, experiments were performed at 37 °C. Upon exposure to fluorescent agonist, FPR appeared mainly internalized as indicated by punctuate green fluorescent intra-cytoplasmic spots (Fig. 3B) which are undetectable in FPR lacking RBL-2H3 cells (not shown). As expected, intra-cytoplasmic spots were prevented by cell pre-incubation with 100 nM fMLF (Fig. 3B). Unlike ARARY that was ineffective, cell pre-exposure to 100 pM pERERY-NH_2 for 30 min strongly reduced internalization in all cell population (Fig. 3B), suggesting a mechanism in which pERERY-NH_2 inhibits cell migration by preventing the agonist-mediated FPR internalization.

Stimulation of RBL-2H3/ETFR cells with fMLF induces activation of several protein kinases, including MAP kinases [21]. As expected, RBL-2H3/ETFR cell exposure to 10 nM fMLF for 5 or 10 min triggered a time-dependent increase of ERK1/2 phosphorylation. Vice versa, cell exposure to 100 pM pERERY-NH_2 for 5 or 10 min, did not affect the basal ERK1/2 phosphorylation, but consistently decreased the amount of fMLF-induced phosphorylated ERK1/2 (Fig. 3C).

Finally, we assessed whether pERERY-NH_2 interferes with the ability of fMLF to evoke an increase in intracellular

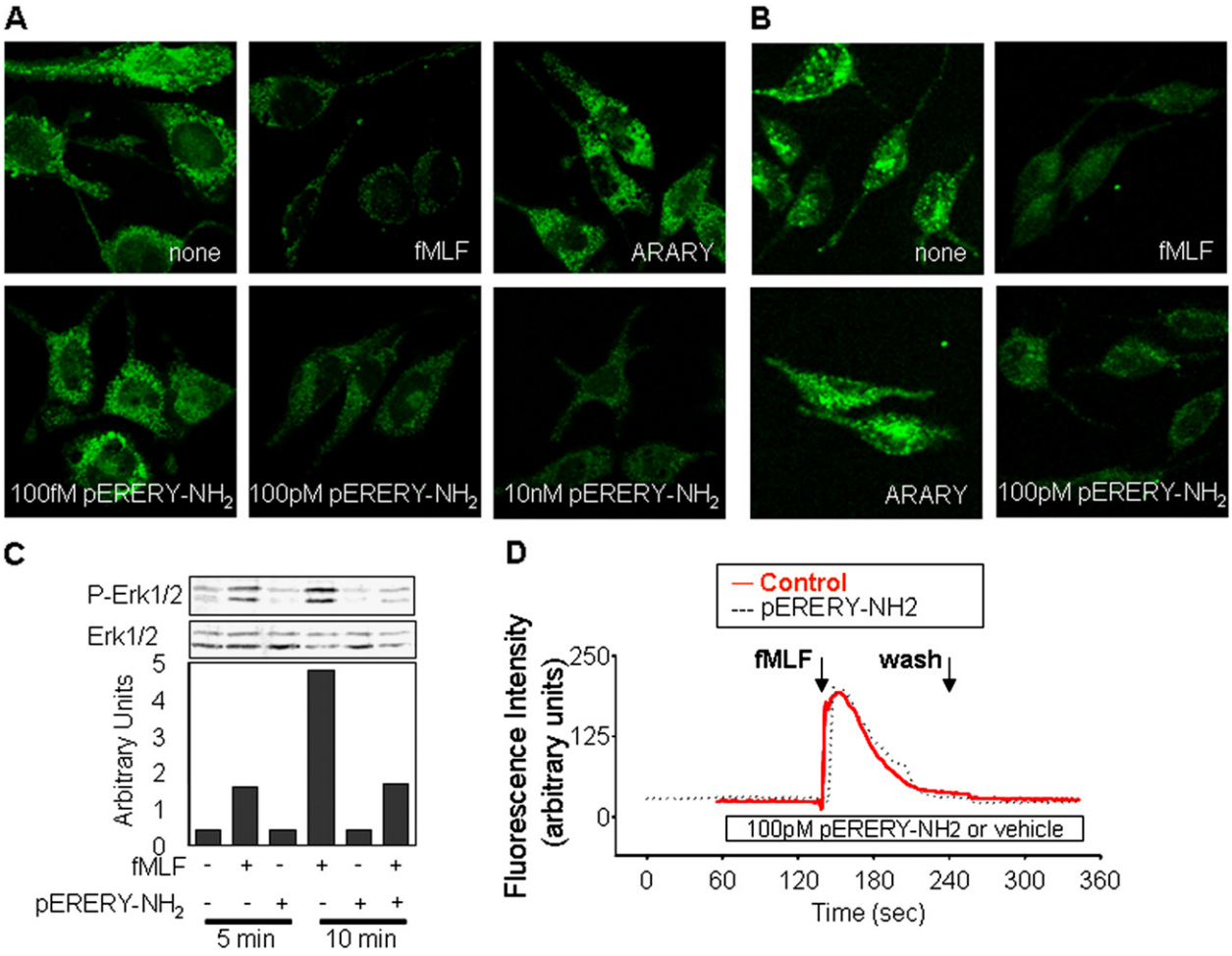

Fig. 3. pERERY-NH_2 inhibits FPR Signaling. Representative confocal images of RBL-2H3/ETFR cells incubated at 4 °C (A) or 37 °C (B) with diluents (none), 100 nM fMLF, 100 pM ARARY or pERERY-NH_2 at the indicated concentrations and then exposed at 4 °C (A) or 37 °C (B) to 10 nM *N*-formyl-Nle-Leu-Phe-Nle-Tyr-Lys fluorescein. Original magnification: 630×. (C) Active (P-ERK1/2) and total ERK1/2 levels in RBL-2H3/ETFR cells exposed to 10 nM fMLF or 100 pM pERERY-NH_2 or diluents, or a combination of 100 pM pERERY-NH_2 and 10 nM fMLF for the indicated times. The histogram shows the OD ratio for P-ERK1/2/ERK1/2 bands as quantified by densitometry. A representative experiment of three is shown. (D) Effect of 100 pM pERERY-NH_2 or vehicle on 10 nM fMLF-induced intracellular Ca^{2+} response. The panel reports, as superimposed traces, the time course of intracellular Ca^{2+} levels, measured as fluo-3 fluorescence intensity, in two different cells, before and after 10 nM fMLF, in the presence of pERERY-NH_2 or vehicle. The traces are representative of 180 cells perfused with vehicle before, during and after the fMLF pulse and 106 cells which after being exposed to Krebs solution during the first minute of recording, were switched to a pERERY-NH_2-containing solution and kept in the presence of this peptide throughout the entire fMLF stimulation and during its washout.

Ca^{2+} concentrations. In control cells, fMLF markedly increased intracellular Ca^{2+} with a rapid peak (mean percentage increase over baseline 577.3 ± 8.2%, $n = 180$ in three different experiments) followed by a plateau maintained until the peptide was washed out (Fig. 3D). pERERY-NH_2 neither modified baseline intracellular Ca^{2+} (fluo3 fluorescence intensity 24.3 ± 1.0 vs. 23.9 ± 1.0, ns) nor the intracellular Ca^{2+} response evoked by further addition of fMLF (mean percentage increase over baseline 595.2 ± 15.7%; $n = 106$ in three different experiments) (Fig. 3D). Overall, our findings indicate that pERERY-NH_2 inhibits SRSRY function by antagonizing FPR-dependent MAP-K activation without interfering with the effects of this receptor on intracellular Ca^{2+} homeostasis.

4. Discussion

We have developed synthetic peptides carrying specific amino acid substitutions along the SRSRY uPAR sequence. Among these, the peptide H-Ser-Arg-Glu-Arg-Tyr-OH was selected for its ability to inhibit SRSRY-directed cell migration. Further modifications led to the generation of the peptide pGlu-Arg-Glu-Arg-Tyr-NH_2 (pERERY-NH_2), which is a potent inhibitor of both SRSRY- and fMLF-directed cell migration. In an effort to characterize the molecular mechanisms underlying the activity of pERERY-NH_2, we demonstrated that pERERY-NH_2 shares the same binding site with SRSRY on the FPR and prevents: (a) binding of a fluorescent fMLF analogue to RBL-2H3/ETFR cell surfaces; (b) fMLF-directed cell migration of RBL-2H3/ETFR cells stably expressing FPR; (c) agonist-dependent FPR internalization and ERK1/2 phosphorylation. These remarkable effects are due to its binding to the FPR.

Many reports clearly show the involvement of the uPAR in cell migration, thus suggesting that this receptor may be regarded as a new molecular target for therapy of diseases sustained by increased cell motility. In this respect, efforts have been made to interfere with the uPA/uPAR or integrin/uPAR interactions [9,21,22]. To the best of our knowledge, pERERY-NH_2 is the first uPAR inhibitor that specifically impairs the uPAR/FPR interaction.

Furthermore, pERERY-NH_2 can be regarded also as a true FPR antagonist. A large body of literature shows that FPRs govern a variety of cellular functions, including chemotaxis which requires ERK1/2 phosphorylation, but not a cytosolic Ca^{2+} increase [23]. In our experiments, pERERY-NH_2 blocks FPR-mediated chemotaxis and ERK1/2 phosphorylation, without affecting intracellular calcium mobilization. Since we have not detected any cell response following exposure to pERERY-NH_2 alone, it is possible that this peptide might behave as a neutral antagonist. pERERY-NH_2 appeared to recognize FPR with a higher affinity (pM) than fMLF or SRSRY (nM) which instead promote chemotaxis. In this respect, pERERY-NH_2 could act as an inverse agonist by shifting, upon binding to FPR, the active state of the receptor toward the inactive one. Regarding the specific affinity of pERERY-NH_2 for its target, competition experiments with a fluorescent fMLF analogue showed that a concentration as low as 100 pM pERERY-NH_2 prevents both internalization and ligand-uptake of FPR. Labelled pERERY-NH_2 is unavailable to us, and therefore we could not determine the affinity of pERERY-NH_2 for the FPR. How pERERY-NH_2 interacts with FPR and what structural basis dictates its high affinity for FPR remain to be investigate. Also, it would be interesting to determine whether pERERY-NH_2 behaves as a neutral antagonist or an inverse agonist for FPR. This issue is relevant in vivo for potential therapeutic applications, since inverse agonist effects are associated with receptor activation and inactivation, whereas neutral antagonism produces no effect when administered alone, but blocks the effects of agonists and inverse agonists [19].

pERERY-NH_2 is a novel FPR antagonist exhibiting a higher affinity as compared with other antagonists of FPR that have been investigated for their putative role as therapeutic agents [24,25]. In particular, the cyclic undecapeptide, cyclosporine H is a potent and selective FPR inverse agonist which prevents both FPR-mediated Ca^{2+} mobilization and chemotaxis [24]. pERERY-NH_2 behaves differently from cyclosporine H because it does not prevent FPR-mediated Ca^{2+} mobilization and it is much more potent than cyclosporine H in inhibiting fMLF-induced chemotaxis ($IC_{50} = 1$ pM and 49 nM, respectively).

GPCRs have a crucial role in the physiopathology of immune system as well as in cancer progression and metastasis. In particular, accumulating evidence suggests that modulating GPCR function might delay the progression of many cancers and their spread to distant organs [26]. Given the finding that pERERY-NH_2 inhibits cell migration by antagonizing FPR, it is reasonable to foresee that this peptide may be employed to develop new drugs for the treatment of diseases that are sustained by a chronic excess of cell migration, such as inflammatory diseases, tumor spread and metastases.

Acknowledgements: We greatly appreciated the gift of rat RBL-2H3 and RBL-2H3/ETFR cells from Prof. Francesco Blasi (DIBIT-Istituto Scientifico San Raffaele, Milan, Italy). We are grateful to Dr. Gioconda Di Carluccio for the technical assistance and to Dr. Davide Viaggiano (Department of Neuroscience, "Federico II" University of Naples, Naples, Italy) for his help in performing time series confocal experiments.

References

[1] Pantel, K. and Brakenhoff, R.H. (2004) Dissecting the metastatic cascade. Nat. Rev. Cancer 4, 448–456.
[2] Chabner, B.A. and Roberts Jr., T.G. (2005) Timeline: chemotherapy and the war on cancer. Nat. Rev. Cancer 5, 65–72.
[3] Blasi, F. and Carmeliet, P. (2002) uPAR: a versatile signaling orchestrator. Nat. Rev. Mol. Biol. 3, 932–943.
[4] Danø, K., Behrendt, N., Høyer-Hansen, G., Johnsen, M., Lund, L.R., Ploug, M. and Rømer, J. (2005) Plasminogen activation and cancer. Thromb. Haemostasis 93, 676–681.
[5] Carriero, M.V., Del Vecchio, S., Capozzoli, M., Franco, P., Fontana, L., Zannetti, A., Botti, G., D'Aiuto, G., Salvatore, M. and Stoppelli, M.P. (1999) Urokinase receptor interacts with alpha(v)beta5 vitronectin receptor, promoting urokinase-dependent cell migration in breast cancer. Cancer Res. 59, 5307–5314.
[6] Ossowski, L. and Aguirre-Ghiso, J.A. (2000) Urokinase receptor and integrin partnership: coordination of signaling for cell adhesion, migration and growth. Curr. Opin. Cell Biol. 12, 613–620.
[7] Cunningham, O., Andolfo, A., Santovito, M.L., Iuzzolino, L., Blasi, F. and Sidenius, N. (2003) Dimerization controls the lipid raft partitioning of uPAR/CD87 and regulates its biological functions. EMBO J. 22, 5994–6003.
[8] Alfano, D., Franco, P., Vocca, I., Gambi, N., Pisa, V., Mancini, A., Caputi, M., Carriero, M.V., Iaccarino, I. and Stoppelli, M.P. (2005) The urokinase plasminogen activator and its receptor: role in cell growth and apoptosis. Thromb. Haemostasis 93, 205–211.

[9] Llinas, P., Le Du, M.H., Gardsvoll, H., Dano, K., Ploug, M., Gilquin, B., Stura, E.A. and Menez, A. (2005) Crystal structure of the human urokinase plasminogen activator receptor bound to an antagonist peptide. EMBO J. 24, 1655–1663.
[10] Barinka, C., Parry, G., Callahan, J., Shaw, D.E., Kuo, A., Bdeir, K., Cines, D.B., Mazar, A. and Lubkowski, J. (2006) Structural basis of interaction between urokinase-type plasminogen activator and its receptor. J. Mol. Biol. 363, 482–495.
[11] Trigwell, S., Wood, L. and Jones, P. (2000) Soluble urokinase receptor promotes cell adhesion and requires tyrosine-92 for activation of p56/59 (hck). Biochem. Biophys. Res. Commun. 278, 440–446.
[12] Gargiulo, L., Longanesi-Cattani, I., Bifulco, K., Franco, P., Raiola, R., Campiglia, P., Greco, P., Peluso, G., Stoppelli, M.P. and Carriero, M.V. (2005) Cross-talk between fMLP and vitronectin receptors triggered by urokinase receptor-derived SRSRY peptide. J. Biol. Chem. 280, 25225–25232.
[13] Resnati, M., Pallavicini, I., Wang, J.M., Oppenheim, J.J., Serhan, C.N., Romano, M. and Blasi, F. (2002) The fibrinolytic receptor for urokinase activates the G protein-coupled chemotactic receptor FPRL1/LXA4R. Proc. Natl. Acad. Sci. USA 99, 1359–1364.
[14] Montuori, N., Carriero, M.V., Salzano, S., Rossi, G. and Ragno, P. (2002) The cleavage of the urokinase receptor regulates its multiple functions. J. Biol. Chem. 277, 46932–46939.
[15] Stewart, J.M. and Young, J.D. (1984) Solid Phase Peptide Synthesis, second ed, Pierce Chemical Company, Rockford.
[16] Le, Y., Gong, W., Tiffany, H.L., Tumanov, A., Nedospasov, S., Shen, W., Dunlop, N.M., Gao, J.L., Murphy, P.M., Oppenheim, J.J. and Wang, J.M. (2001) Amyloid (beta)42 activates a G-protein-coupled chemoattractant receptor, FPR-like-1. J. Neurosci. 21, RC123.
[17] Franco, P., Vocca, I., Carriero, M.V., Alfano, D., Cito, L., Longanesi-Cattani, I., Grieco, P., Ossowski, L. and Stoppelli, M.P. (2006) Activation of urokinase receptor by a novel interaction between the connecting peptide region of urokinase and alpha v beta 5 integrin. J. Cell Sci. 119, 3424–3434.
[18] Carriero, M.V., Del Vecchio, S., Franco, P., Potena, M.I., Chiaradonna, F., Botti, G., Stoppelli, M.P. and Salvatore, M. (1997) Vitronectin binding to urokinase receptor in human breast cancer. Clin. Cancer Res. 3, 1289–1308.
[19] Perez, D.M. and Karnik, S.S. (2005) Multiple signaling states of G-protein-coupled receptors. Pharmacol. Rev. 57, 147–161.
[20] Bennett, T.A., Maestas, D.C. and Prossnitz, E.R. (2000) Arrestin binding to the G protein-coupled *N*-formyl peptide receptor is regulated by the conserved "DRY" sequence. J. Biol. Chem. 275, 24590–24594.
[21] Duffy, M.J. (2004) The urokinase plasminogen activator system: role in malignancy. Curr. Pharm. Des. 10, 39–49.
[22] Degryse, B., Resnati, M., Czekay, R.P., Loskutoff, D.J. and Blasi, F. (2005) Domain 2 of the urokinase receptor contains an integrin-interacting epitope with intrinsic signaling activity: generation of a new integrin inhibitor. J. Biol. Chem. 280, 24792–24803.
[23] Bae, Y.S., Song, J.Y., Kim, Y., He, R., Ye, R.D., Kwak, J.Y., Suh, P.G. and Ryu, S.H. (2003) Differential activation of formyl peptide receptor signaling by peptide ligands. Mol. Pharmacol. 64, 841–847.
[24] Yan, P., Nanamori, M., Sun, M., Zhou, C., Cheng, N., Li, N., Zheng, W., Xiao, L., Xie, X., Ye, R.D. and Wang, M.W. (2006) The immunosuppressant cyclosporin A antagonizes human formyl peptide receptor through inhibition of cognate ligand binding. J. Immunol. 177, 7050–7058.
[25] Bae, Y.S., Lee, H.Y., Jo, E.J., Kim, J.I., Kang, H.K., Ye, R.D., Kwak, J.Y. and Ryu, S.H. (2004) Identification of peptides that antagonize formyl peptide receptor-like 1-mediated signaling. J. Immunol. 173, 607–614.
[26] Dorsam, R.T. and Gutkind, J.S. (2007) G-protein-coupled receptors and cancer. Nat. Rev. Cancer 7, 79–94.